Int. J. Solids Structures Vol. 21, No. 10, pp. 1025–1034, 1985
Printed in Great Britain.

0020-7683/85 \$3.00+.00

THE CRUCIFORM CRACK RUNNING IN A BIAXIAL TENSION FIELD

L. M. BROCK and Y. C. DENG†
Engineering Mechanics, University of Kentucky, Lexington, KY 40506, U.S.A.

(*Received* 28 *March* 1984; *in revised form* 16 *October* 1984)

Abstract—Under a biaxial tension field, failure in a small region can give rise to simultaneous rapid crack extension along multiple paths. To gain insight into this phenomenon, the dynamic analysis of a cruciform crack growing from a point in a biaxial tension field is considered. An analytic solution is at present not available. However, by treating the cruciform arms as dislocation arrays, the problem is reduced to a pair of coupled integral equations. By following a scheme for plane crack analysis, these equations are uncoupled, and solved numerically by a standard technique for singular integral equations. Examination of the solution indicates that a plane crack is more likely to occur than a cruciform crack in a uniform biaxial tension field, and the crack openings will be larger.

INTRODUCTION

The rapid branching of cracks from a main crack has received much attention recently[1–4]. In a biaxial tension field, however, rapid crack extension may occur simultaneously along multiple paths radiating from a single localized failure initiation region. An important example arises in projectile impacts on stressed panels[5]. To gain insight into this phenomenon, we here consider a cruciform crack growing from a point in an unbounded plane subjected to a biaxial tension field. The plane is linearly elastic, isotropic, and homogeneous, and each collinear pair of arms in the cruciform extends symmetrically at a constant subcritical speed.

The quasi-static problem of a fixed-length cruciform crack is solvable by standard analytical methods[6]. However, fully dynamic analytical solutions to problems of in-plane tractions specified on crack surfaces which meet at right angles are not presently available[7]. Therefore it is important that the solution approach adopted allow a straightforward and efficient numerical treatment. In this light, the cruciform arms are here viewed as dislocation arrays distributed with respect to speed. This idea has been used extensively[8–11] for dynamic fracture problems. In particular, [11] treated a cruciform crack driven by normal point forces moving along the crack surfaces.

As a first step in the problem solution, therefore, the next section considers a general problem of dislocation arrays moving at constant speeds in opposite directions from a point. In the following section the cruciform crack problem is formulated, and the dislocation solution is used to reduce the problem to coupled singular integral equations. In subsequent sections these are decoupled and easily solved numerically. A special case of the solution is used to study the dynamic stress intensity factors, energy release rates and crack openings, and to compare them with those for a plane crack.

DISLOCATIONS IN AN UNBOUNDED PLANE

For $s \le 0$, where s is the time multiplied by the dilatational wave speed, an unbounded plane is at rest. For $s > 0$, dislocations of strength

$$n!\,(s - |y|/c)^n \tag{1}$$

† Present address: General Motors Research Laboratories, Warren, MI 48090, U.S.A.

extend by climb in both directions from the point $(x, y) = 0$ along the y-axis at a constant nondimensionalized speed $c > 0$. Here the integer $n \geq 0$, (x, y) are the Cartesian coordinates, and all speeds are nondimensionalized by dividing by the dilatational wave speed. Dislocations extending along arbitrary paths at arbitrary speeds by both climb and glide in an unbounded plane have been considered in [12]. Using that work and the x- and y-symmetry of the present problem, it is easily shown for $n = 0$ that the normal stresses along, respectively, the positive y- and x-axes are

$$\frac{\pi}{\mu} m^2 y\sigma_x = A_1(t, k)H(t - 1) + A_m(t, k)H(t - m), \tag{2}$$

$$\frac{\pi}{\mu} m^2 x\sigma_y = B_1(t, k)H(t - 1) + B_m(t, k)H(t - m), \tag{3}$$

where $k = 1/c$, $t = s/y$ and $t = s/x$ in (2) and (3), respectively, and

$$A_1 = \frac{T^2}{2a}\left(\frac{1}{t - k} - \frac{1}{t + k}\right), \qquad A_m = -2bt^2\left(\frac{1}{t - k} - \frac{1}{t + k}\right), \tag{4}$$

$$a(k^2 + a^2)B_1 = kTM, \qquad (k^2 + b^2)B_m = -4t^2bk, \tag{5}$$

$$T = 2t^2 - m^2, \qquad M = 2a^2 + m^2, \qquad a = \sqrt{(t^2 - 1)}, \qquad b = \sqrt{(t^2 - m^2)}. \tag{6}$$

Here $H(\ )$ is the Heaviside function, μ is the shear modulus, and 1 and $1/m$ are the nondimensionalized dilatational and rotational wave speeds. For $n > 0$, (2) and (3) are replaced by

$$\frac{\pi}{\mu}\frac{m^2}{n}\sigma_x = \int_1^t A_1(q, k)(s - qy)^{n-1}\,dq + \int_m^t A_m(q, k)(s - qy)^{n-1}\,dq, \tag{7}$$

$$\frac{\pi}{\mu}\frac{m^2}{n}\sigma_y = \int_1^t B_1(q, k)(s - qx)^{n-1}\,dq + \int_m^t B_m(q, k)(s - qx)^{n-1}\,dq. \tag{8}$$

It should be noted that the first and second terms in A_1 are due to the dilatational waves radiating from the dislocation edge $y = cs$ and reflections from the edge $y = -cs$, respectively. The two terms in A_m are the rotational wave counterparts. These wave pairs are combined in B_1 and B_m.

If Δu and Δv are the discontinuities in the normal displacement in going from, respectively, $x = 0-$ to $x = 0+$ across the positive y-axis and $y = 0-$ to $y = 0+$ across the positive x-axis, then clearly

$$\Delta u = n!(s - ky)^n H(t - k), \qquad \Delta v = 0. \tag{9}$$

Equations (1)–(9) show that the dislocation problem displacements are homogeneous of degree n in (x, y, s). Suppose now that the dislocations are replaced by continuous arrays of dislocations whose nondimensionalized speeds are constants in the range $(0, c)$, and whose strengths are characterized by their speed. Moreover, suppose that the resulting solution is also to exhibit x- and y-symmetry and displacement homogeneity of degree n. It is readily shown by superposition then that eqn (9) would be replaced by

$$\Delta u = n!\int_k^t F(p)(s - py)^n\,dp, \qquad \Delta v = 0 \tag{10}$$

where $F(p)$ is the characterization function, here defined in terms of inverse speed. Equation (10) can also be viewed as the result of the (x, y, s)-independent operation

$$\int_k^\infty (\ )F(p)\,dp. \tag{11}$$

Indeed, any field variable for the dislocation array problem can be obtained by operating on the corresponding field variable for the dislocation problem with eqn (11).

The dislocation array problem gives, in effect, a solution representation for a general problem which exhibits x- and y-symmetry, displacements of nth degree homogeneity in (x, y, s) and involves no disturbance except a normal displacement discontinuity, which extends in opposite directions with nondimensionalized speed c along the y-axis away from the origin and vanishes at its edges for $n > 0$. A particular solution depends on the choice of $F(p)$.

THE CRUCIFORM CRACK

Consider an unbounded plane in equilibrium for $s < 0$ under a uniform biaxial stress field defined in terms of Cartesian coordinates by

$$\sigma_x = \sigma_1, \qquad \sigma_y = \sigma_2, \qquad \sigma_{xy} = 0 \qquad (\sigma_i > 0). \tag{12}$$

At $s = 0$, failure occurs at the origin $(x, y) = 0$ and cracks extend in both directions along the y- and x-axes at the constant nondimensionalized subcritical speeds c_1 and c_2, respectively. The loading, crack and wave pattern for $s \geq 0$ are shown in Fig. 1. The solution to this problem can be obtained by superposing the equilibrium solution arising from eqns (12) and the solution to the problem of the same cracks extending for $s \geq 0$ in a stress-free plane with surfaces subjected to the negatives of (12). This latter problem has no characteristic length, and it can therefore be determined[13] that the displacements are homogeneous of degree 1 in (x, y, s). Equations (12) guarantee that the solutions will exhibit x- and y-symmetry. The cracks induce discontinuities in the normal displacements which propagate in both directions along the x- and y-axes. Moreover, these discontinuities vanish at the crack edges.

Comparison of these properties with those noted in the previous section show that the solution to this problem can be represented by a *superposition* of the dislocation-array solutions for $n = 1$, *where one solution has the roles of* $(\Delta u, \Delta v)$ *and* (σ_x, σ_y)

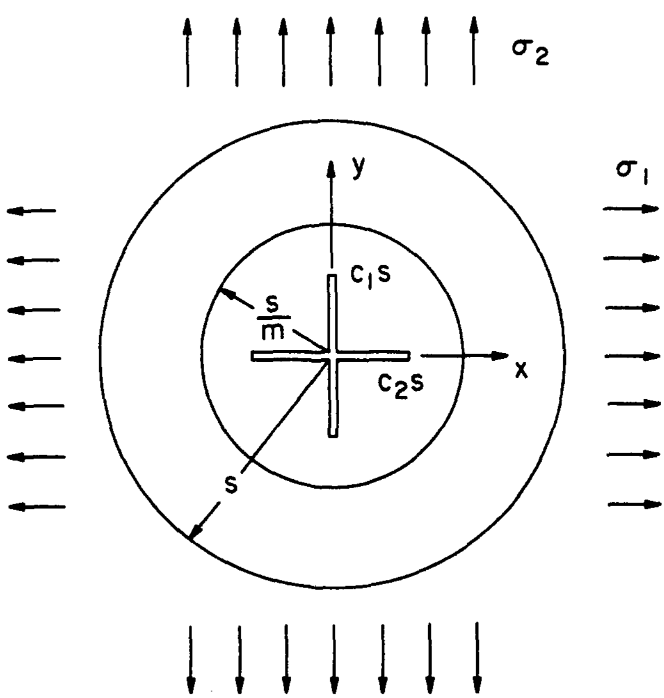

Fig. 1. Wave pattern cruciform crack in uniform biaxial tension.

reversed. That is, eqns (8)–(10) give in view of (11)

$$\Delta u = \int_{k_1}^{t} F_1(p)(s - py)\,\mathrm{d}p, \tag{13}$$

$$\frac{\pi}{\mu} m^2\sigma_x = \int_{k_1}^{\infty} F_1(p)\left[\int_1^t A_1(q, p)\,\mathrm{d}p + \int_m^t A_m(q, p)\,\mathrm{d}q\right]\mathrm{d}p$$
$$- \int_{k_2}^{\infty} F_2(p)\left[\int_1^t B_1(q, p)\,\mathrm{d}q + \int_m^t B_m(q, p)\,\mathrm{d}q\right]\mathrm{d}p \tag{14}$$

along the positive y-axis, where $t = s/y$ and $k_i = 1/c_i$. Analogous expressions hold for Δv and σ_y along the positive x-axis, with the roles of (F_1, F_2), (x, y) and (k_1, k_2) reversed. The problem analysis thus reduces to finding the characterization functions F_i so that

$$\sigma_x = -\sigma_1, \qquad \sigma_y = -\sigma_2, \tag{15}$$

for $x = 0$, $0 < y < c_1 s$ and $y = 0$, $0 < x < c_2 s$, respectively. Problem symmetry guarantees that (15) and the condition $\sigma_{xy} = 0$ will be satisfied for $x = 0$, $|y| < c_1 s$ and $y = 0$, $|x| < c_2 s$.

Substitution of (14) and its σ_y-analog in (15), recognizing that the aforementioned symmetry also implies $F_i(p) = F_i(-p)$ and employing the more convenient quantities c_i and

$$G_i(u)u = F_i(p), \qquad z = 1/t, \qquad u = 1/p, \qquad v = 1/q \tag{16}$$

yields the results

$$\int_i G_i(u)A(u, z)\,\mathrm{d}u + \int_j G_j(u)B(u, z)\,\mathrm{d}u = -\frac{m^2}{\mu}\pi\sigma_i \qquad (0 < z < c_i), \tag{17}$$

where it is understood that $i = (1, 2)$ when $j = (2, 1)$, $\int_i$ denotes integration over the range $(-c_i, c_i)$ and

$$A = \int_z^1 \frac{A_1(v)}{u - v}\,\mathrm{d}v + \int_z^{1/m} \frac{A_m(v)}{u - v}\,\mathrm{d}v, \quad B = \int_z^1 \frac{B_1(v)}{v^2 + u^2a^2}\,\mathrm{d}v + \int_z^{1/m} \frac{B_m(v)}{v^2 + u^2b^2}\,\mathrm{d}v. \tag{18}$$

In (18) the quantities (A_1, A_m, B_1, B_m) are now defined by

$$A_1 = \frac{T^2}{2av^4}, \qquad A_m = -\frac{2b}{v^4}, \qquad B_1 = \frac{-MT}{2av^3}, \qquad B_m = \frac{2b}{v^3} \tag{19}$$

$$T = 2 - m^2v^2, \qquad M = 2a^2 + m^2v^2, \qquad a = \surd(1 - v^2), \qquad b = \surd(1 - m^2v^2) \tag{20}$$

and the A-integrations must be performed in the Cauchy principal value sense in eqn (17).

Equation (17) defines a pair of coupled integral equations for the functions G_i. Double integration and singular integrals of the Cauchy type are involved, and an analytic solution is not presently available. However, by following an approach[13] for the analytic solution of plane crack problems, the equations can be rewritten in a manner which leads to extraction of the singular integrals from double integration and decoupling.

The decoupled equations also cannot at present be solved analytically, but are similar in form to equations for a plane crack for which an analytic solution is known. Therefore a numerical scheme can be devised which corresponds to the analytical procedure. Moreover, this scheme involves a standard technique developed for singular integral equations in quasi-static problems[14].

EQUATION DECOUPLING

Following [13], it is seen that unless the v-integration contribution in eqn (17) from the range (z, c_i) vanishes, the left-hand side will not give a constant value. Consequently, it is only the contributions from the ranges $(c_i, 1)$ and $(c_i, 1/m)$ that give the particular constant on the right-hand side. Equation (17) can therefore be replaced by the coupled equation pair

$$\fint_i \frac{G_i(u)}{u - v}\,du + \int_j G_j(u)C(u, v)\,du = 0 \qquad (0 < v < c_i), \tag{21}$$

$$\int_i G_i(u)A(u, c_i)\,du + \int_j G_j(u)B(u, c_i)\,du = -\frac{m^2}{\mu}\pi\sigma_i, \tag{22}$$

where

$$C(u, v) = \frac{v}{R}\left(\frac{MT}{v^2 + u^2a^2} - \frac{4ab}{v^2 + u^2b^2}\right), \qquad R = 4ab - T^2 \tag{23}$$

and $\fint$ denotes principal value integration. Here R is the Rayleigh function, and has a double root at $v = 0$ and roots at $v = \pm$(nondimensionalized Rayleigh wave speed). However, it can be shown that $C(u, 0) = 0$, while the subcritical crack edge speeds considered here mean that v cannot assume Rayleigh speed values in eqns (21) and (22).

Equation (21) can be viewed as an inhomogeneous singular Fredholm integral equation of the first kind for G_i. A formal solution[15] readily yields an expression for G_i in terms of G_j. Substitution of this expression with the indices interchanged in eqns (21) and (22), and performing the indicated u-integrations then yields the uncoupled equation pair

$$\fint_i G_i(u)\left[\frac{1}{u - v} - C_j(u, v)\right]du = 0 \qquad (0 < v < c_i), \tag{24}$$

$$\int_i G_i(u)\,[A(u, c_i) - D_j(u)]\,du = -\frac{m^2}{\mu}\pi\sigma_i, \tag{25}$$

where the functions D_j and C_j are defined by

$$D_j(u) = \int_{c_i}^{1} B_1(v)A_{ij}(v, u)\,dv + \int_{c_i}^{1/m} B_m(v)B_{ij}(v, u)\,dv, \tag{26}$$

$$C_j(u, v) = \frac{v}{R}\,[MTA_{ij}(v, u) - 4abB_{ij}(v, u)], \tag{27}$$

$$\surd(v^2 + a^2c_j^2)^3 A_{ij}(v, u) = \frac{v}{\pi}\int_i \frac{C(u, w)\surd(c_i^2 - w^2)^3}{v^2 + a^2w^2}\frac{dw}{w}, \tag{28}$$

and B_{ij} follows from (28) by replacing a with b.

NUMERICAL SOLUTION

Setting $(c_j, \sigma_j) = 0$ reduces eqns (24) and (25) to

$$\fint_i \frac{G_i(u)}{u - v}\,du = 0 \qquad (0 < v < c_i), \tag{29a}$$

$$\int_i G_i(u)A(u, c_i)\,du = -\frac{m^2}{\mu}\pi\sigma_i, \tag{29b}$$

where $i = 1$ or $i = 2$. Equation (29) is clearly that for a plane crack, and the analytic solution essentially proceeds as follows: In view of boundedness requirements as $|u| \to \infty$, the homogeneous condition (29a) can be solved for G_i to within an arbitrary constant factor[15]. The factor can then be determined by substituting the (29a) solution into (29b). The result is

$$G_i = -\frac{m^2\pi}{I(c_i)}\frac{\sigma_i}{\mu}\frac{u^2}{\sqrt{(c_i^2 - u^2)^3}}, \tag{30}$$

$$I(c) = -2\frac{m^2}{c^2}K(b) + \frac{1}{2c^2}\left(m^4c^2 + \frac{T^2}{a^2}\right)K(a) - \frac{1}{2c^4}\left(4 + \frac{T^2}{a^2}\right)E(a) + \frac{4}{c^2}E(b), \tag{31}$$

where (T, a, b) as defined by eqn (20) are functions of c while (K, E) are complete elliptic integrals of the first and second kind of the arguments in parentheses.

This analytical procedure suggests the following numerical solution scheme for (24) and (25): Based on the form of eqn (30), the substitutions

$$G_i = -\frac{m^2}{\mu}P_i\sigma_i\left[\frac{u^2}{c_i^2 - u^2} + g_i(U)\right]\frac{1}{\sqrt{(c_i^2 - u^2)}}, \qquad U = \frac{u}{c_i}, \qquad V = \frac{v}{c_i} \tag{32}$$

are made, whereupon eqns (24) and (25) become

$$⨍ g_i(U)\left[\frac{1}{U - V} - c_iC_j(c_iU, c_iV)\right]\frac{\mathrm{d}U}{\sqrt{(1 - U^2)}} = L_i(c_iV) \qquad (0 < V < 1), \tag{33}$$

$$\int g_i(U)[A(c_iU, c_i) - D_j(c_iU)]\frac{\mathrm{d}U}{\sqrt{(1 - U^2)}} - J_i = \frac{\pi}{P_i}, \tag{34}$$

$$L_i(v) = 2c_i\int_i C_i'(c_j, w)\frac{v^4a(v)}{R(v)}[B_1'(v, w) + B_m'(v, w)]\,\mathrm{d}w, \tag{35}$$

$$J_i = \int_i C_i'(c_j, w)\left[\int_{c_i}^{1} B_1'(v, w)\,\mathrm{d}v + \int_{c_i}^{1/m} B_m'(v, w)\,\mathrm{d}v\right]\mathrm{d}w, \tag{36}$$

$$RC_i'(u, w) = \left[\frac{MT}{\sqrt{(w^2 + a^2u^2)^3}} - \frac{4ab}{\sqrt{(w^2 + b^2u^2)^3}}\right]w\sqrt{(c_i^2 - w^2)^3}, \tag{37}$$

$$(v^2 + a^2w^2)\sqrt{(v^2 + a^2c_i^2)^3}B_1'(v, w) = vB_1(v), \tag{38}$$

where $B_m'(v, w)$ follows from eqn (38) by replacing a with b and the subscript 1 with m, and it is understood that $\int$ implies integration over the range $(-1, 1)$. The L_i and J_i-terms arise from performing the integrations involving the first term in the expression for G_i. The remaining U-integrations can formally be approximated by Chebyshev–Gauss[16] quadrature so that eqns (33) and (34) are replaced by

$$\frac{2\pi}{N}\sum g_i(U_\alpha)P_{i\alpha}(V) = L_i(c_iV) \qquad (0 < V < 1), \tag{39a}$$

$$\frac{2\pi}{N}\sum g_{i\alpha}(U_\alpha)Q_{i\alpha} - J_i = \frac{\pi}{P_i} \tag{39b}$$

$$P_{i\alpha}(V) = \frac{V}{U_\alpha^2 - V^2} - c_iC_j(c_iU_\alpha, c_iV), \qquad Q_{i\alpha} = D_A(c_iU_\alpha, c_i) - D_j(c_iU_\alpha) \tag{40}$$

$$U_\alpha = \cos\frac{\pi}{2N}(2\alpha - 1) \tag{41}$$

where $\sum$ denotes summation on the integer α over the range $(1, N/2)$, $N > 1$ is an even integer and problem symmetry requires that $g_i(U) = g_i(-U)$ while $U_\alpha =$

$-U_{N+1-\alpha}$. The term D_A follows from integrating A as

$$D_A(u, c) = \frac{A_1}{2}\ln\frac{a - a(c)}{a + a(c)} - \frac{1}{2u^4}(T + u^2)\ln\frac{1 - a(c)}{1 + a(c)} + \frac{a(c) - b(c)}{u^2c^2} + \frac{A_m}{2}\ln\frac{b - b(c)}{b + b(c)} + \frac{T}{2u^4}\ln\frac{1 - b(c)}{1 + b(c)} \quad (42)$$

where the u-independence is understood unless explicity indicated otherwise.

By satisfying eqn (33) at the $N/2$ collocation points $V = V_\beta$, where

$$V_\beta = \cos\frac{\pi\beta}{N} \qquad (\beta = 1, 2, \ldots, N/2) \quad (43)$$

and $0 < V_\beta < 1$, eqn (39a) yields a set of $N/2$ linear algebraic equations for the $N/2$ unknown values $g_i(U_\alpha)$. These can then be substituted into (39b) to find the constant P_i, so that an approximation to G_i can be constructed. The equation set arising from (39a) is efficiently solved by Gaussian elimination because, although $U_\alpha \neq V_\beta$, the lead term in $P_{i\alpha}$ gives a coefficient matrix with dominant diagonal elements, while the integrations (A_{ij}, B_{ij}, L_i, J_i) are well-behaved and easily performed numerically.

CRACK OPENING AND STRESS-INTENSITY FACTOR

Because the equilibrium solution involves no crack, the crack openings W_1 and W_2 along the positive y- and x-axes, respectively, are found from eqns (13), (16) and (32) to be

$$\frac{c_i}{m^2}\frac{\mu}{\sigma_i}\frac{W_i}{s} = P_i\left[\sqrt{(1 - Z^2)} - \int_Z^1 \frac{g_i(U)(U - Z)}{U^2\sqrt{(1 - U^2)}}\,dU\right], \quad (44a)$$

$$Z = \frac{z}{c_i} \quad (44b)$$

where $i = (1, 2)$. Similarly, from eqns (14) and (16) the normal stresses S_1 and S_2 along these axes ahead ($z > c_i$) of the crack edges are obtained as

$$\begin{aligned} S_i = &-\frac{1}{\pi}\int [P_i\sigma_i g_i(U)A(c_iU, z) + P_j\sigma_j g_j(U)B(c_jU, z)]\frac{dU}{\sqrt{(1 - U^2)}} \\ &+ P_j\sigma_j\left[\int_z^1 \frac{vB_1(v)\,dv}{\sqrt{(v^2 + a^2c_j^2)^3}} + \int_z^{1/m}\frac{vB_m(v)\,dv}{\sqrt{(v^2 + b^2c_j^2)^3}}\right] \\ &- P_i\sigma_i I'(c_i, z) + \frac{2}{c_i^4 z}P_i\sigma_i(b' - a')\sqrt{(z^2 - c_i^2)} \\ &+ \frac{z}{2c_i^4}P_i\sigma_i\left[4b' - T^2(c_i)\frac{a'}{1 - c_i^2}\right]\frac{1}{\sqrt{(z^2 - c_i^2)}}, \end{aligned} \quad (45)$$

$$a' = a(z)H(1 - z), \qquad b' = b(z)H(1 - mz) \quad (46)$$

where $i = (1, 2)$ when $j = (2, 1)$ while $I'(c, z)$ follows from $I(c)$ by replacing the complete elliptic integrals $K(a)$, $K(b)$, $E(a)$ and $E(b)$ with

$$F(a, \lambda_a)H(1 - z), \quad F(b, \lambda_b)H(1 - mz), \quad E(a, \lambda_a)H(1 - z), \quad E(b, \lambda_b)H(1 - mz), \quad (47)$$

respectively. Here $F(u, v)$ and $E(u, v)$ are incomplete elliptic integrals of the first and second kind of modulus u and argument v, and (a, b) are understood to be functions of c unless specified otherwise. The arguments are defined by

$$a \sin \lambda_a = a(z), \qquad b \sin \lambda_b = b(z). \tag{48}$$

The v-integrations in eqn (45) are easily performed numerically, while the U-integrations can be approximated by Chebyshev–Gaussian quadrature as

$$-\frac{2}{N} P_i\sigma_i \sum g_i(U_\alpha)D_A(z, c_iU_\alpha) - \frac{2}{N} P_j\sigma_j \sum g_j(U_\alpha)D_B(z, c_jU_\alpha), \tag{49}$$

$$D_B(u, c) = \frac{B_1}{2u} \ln \frac{1 + a(c)a}{1 - a(c)a} - \frac{1}{2u^4}(2 - u^2) \ln \frac{1 - a(c)}{1 + a(c)}$$
$$+ \frac{b(c) - a(c)}{u^2c^2} + \frac{A_m}{2} \ln \frac{1 - b(c)b}{1 + b(c)b} + \frac{T}{2u^4} \ln \frac{1 - b(c)}{1 + b(c)}. \tag{50}$$

Introduction of eqn (49) allows S_i to be calculated in terms of the collocation values $g_i(U_\alpha)$.

Study of (49) shows that the last term in (45) is singular as $z \to c_i+$. It is then easily shown that

$$S_i \sim \frac{\sigma_i K_{Ii}}{\surd(z - c_i)}, \tag{51a}$$

$$K_{Ii} = \frac{P_i R(c_i)}{\surd(2c_i)^3 c_i^2 a(c_i)} \tag{51b}$$

as $z \to c_i+$, where K_{Ii} is the mode-I dynamic stress intensity factor. It is noted that K_{Ii} vanishes when c_i reaches the Rayleigh wave speed, as for the plane crack[17].

For a plane crack extending along either the positive y- or x-axis with nondimensionalized subcritical speed c in the uniform plane hydrostatic tension field $\sigma_1 = \sigma_2 = \sigma$, it is easily shown[13] that eqns (44a) and (51b) are replaced by

$$\frac{c}{m^2} \frac{\mu}{\sigma} \frac{W}{s} = \frac{\pi}{I(c)} \surd(1 - Z^2), \tag{52a}$$

$$K_I = \frac{\pi R(c)}{\surd(2c)^3 c^2 a(c) I(c)}, \tag{52b}$$

$$Z = \frac{z}{c}, \tag{52c}$$

where I is defined by eqn (31). For insight into cruciform crack opening and dynamic stress intensity factor behavior—and how it compares with that for the plane crack—eqns (44a) and (51a) are plotted in Fig. 2(a) and eqns (51b) and (52b) are plotted in Fig. 2(b) for the special case $c_1 = c_2 = c$, $\sigma_1 = \sigma_2 = \sigma$. Here the symbols (+) and (−) refer to the cruciform and plane crack quantities, respectively, while m is given the typical value $\surd 3$, which means that the nondimensionalized Rayleigh speed has the value 0.5308.

Figures 2(a) and 2(b) show that the cruciform crack quantities vary in much the same manner as those for the plane crack with respect to crack edge speed and the dynamic similarity variable Z. Several differences, however, are apparent:

The plane crack intensity factor for a given crack speed and the plane crack opening for a given Z are always greater, although the differences diminish with increasing crack speed. Moreover, the W-curve slopes indicate that the cruciform crack surface has a more wedge-like profile. The W-behavior differences may follow from the fact that, in the cruciform crack, the collinear tensile stress tends to close through the

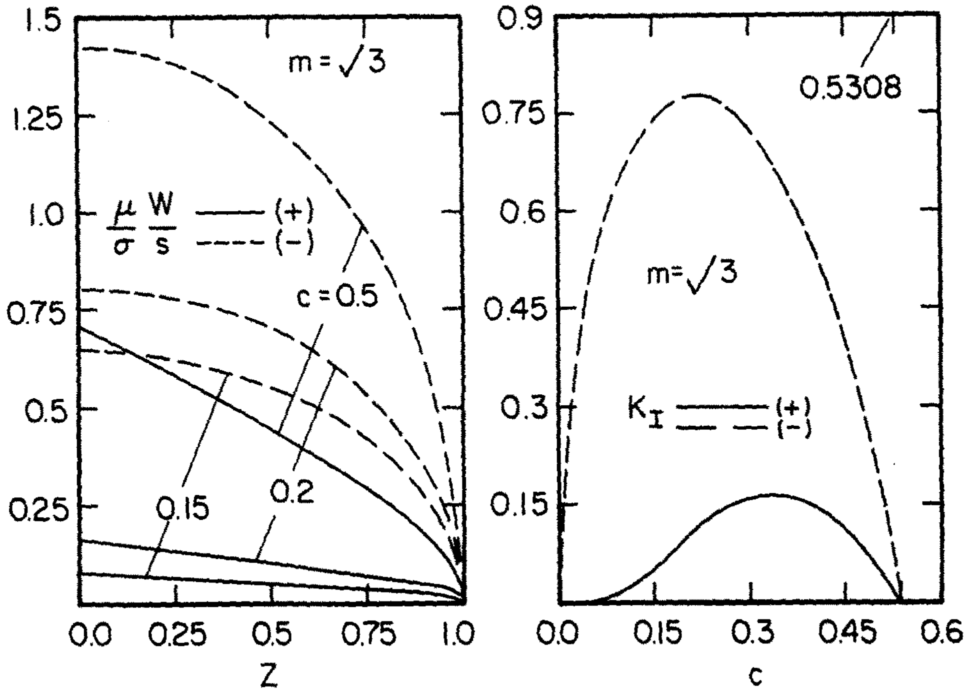

Fig. 2. (a) Crack openings for cruciform (+) and plane (−) cracks. (b) Dynamic stress intensity factors for cruciform (+) and plane (−) cracks.

Poisson effect a particular crack arm. The intensity factor differences agree with quasi-static results for a cruciform crack hydrostatic tension configuration in uniform uniaxial anti-plane shear[18]. Thus, a fracture toughness criterion would predict that a plane crack is more likely to extend in a uniform plane hydrostatic tension field than are the collinear arms of a cruciform crack.

Fracture criteria are also often based on the energy release rate[19]. It is easily shown that the total rate (per unit of out-of-plane length) for the cruciform crack, denoted here by $\dot{E}_C$, can be obtained from eqns (44) and (51) as

$$\dot{E}_c = 2\pi s \frac{m^2}{\mu}\left[\frac{a(c_1)}{R(c_1)}\sigma_1^2 K_{I1}^2 c_1^3 + \frac{a(c_2)}{R(c_2)}\sigma_2^2 K_{I2}^2 c_2^3\right]. \tag{53}$$

The corresponding quantity for the plane crack follows merely by removing one of the terms in brackets and dropping the nonroman subscripts on the remaining term. The ratio of these rates for the special case treated above is then

$$\dot{E}_c^+/\dot{E}_c^- = 2(K_I^+/K_I^-)^2. \tag{54}$$

In view of Fig. 2(b), eqn (54) indicates that the plane crack extension is associated with larger release rates than is the cruciform crack in the uniform plane hydrostatic tension field.

SUMMARY

The results derived here suggest that plane crack extension is, at once, more likely to occur and more likely to generate larger crack openings than a cruciform crack for the special tension field considered. To be sure, these results are for constant-speed rectilinear extension. Moreover, the special field in itself has no preferred crack extension direction. However, the fracture scenario presented here assumed sudden catastrophic failure initiation in a localized region, e.g. [5]. In such circumstances, fracture is almost instantaneous, its initial direction is largely determined by local effects, and it proceeds for a time in this direction at a rapid, nearly constant speed.

The plane crack results, often used here, are contained in a special case in the results of [13]. The plane crack problem was first solved by Broberg[20], of course. However, the method and form of the solutions in [13] were more convenient for purposes of the present analysis.

It should be noted that the cruciform crack does not mathematically reduce to the plane crack case merely by removing σ_1 or σ_2 due to Poisson's ratio coupling between the normal stresses σ_x and σ_y. As in most fracture analysis, it is a mathematical model with an assumed geometry; the validity of basic geometrical details may depend on the additional conditions imposed on the mathematical analysis in view of fracture criteria.

It should also be noted that the dynamic stress intensity factor and crack opening values obtained here varied by no more than 1% when the number of collocation points reached 14 ($N = 30$). One reason for this efficiency was that, as in [11], the unknown characterization function G_i was resolved into a component which had essentially the plane crack solution form and an unknown correction function, g_i. The plane crack solution form carried the crack edge singularity in the solution field. Therefore, the function g_i could act as a nonsingular perturbation although, clearly, its effect on the solution field through the factor P_i is not a perturbation in the often-used sense of the term. The solution scheme adopted here can be used for problems in which the displacements have a degree of homogeneity greater than 1.

REFERENCES

1. J. D. Achenbach and V. K. Varatharajulu, Skew crack propagation at the diffraction of a transient stress wave. *Q. Appl. Math.* **32**, 123–135 (1974).
2. P. Burgers and J. P. Dempsey, Two analytical solutions for dynamic crack bifurcation in anti-plane strain. *J. Appl. Mech.* **49**, 366–370 (1982).
3. P. Burgers, Dynamic propagation of a kinked or bifurcated crack in anti-plane strain. *J. Appl. Mech.* **49**, 371–376 (1982).
4. J. P. Dempsey, M.-K. Kuo and J. D. Achenbach, Mode III crack kinking under stress-wave loading. *Wave Motion* **4**, 181–190 (1982).
5. J. F. Lundeberg and R. J. Bristow, Gunfire damage to airframe structures. *AIAA* Paper No. 66-783 (1966).
6. M. P. Stallybrass, A pressurized crack in the form of a cross. *Q. J. Mech. Appl. Math.* **23**, 35–48 (1969).
7. J. Miklowitz, Wavefront analysis in nonseparable elastodynamic quarter plane problems, I, Part 1: The general method. *J. Appl. Mech.* **49**, 797–807 (1982).
8. L. B. Freund, The stress intensity factor due to normal impact loading of the faces of a crack. *Int. J. Eng. Sci.* **12**, 179–190 (1974).
9. P. Burgers and L. B. Freund, An addendum to the paper: dynamic growth of an edge crack in a half-space. *Int. J. Solids Struct.* **17**, 721–727 (1981).
10. L. M. Brock, Shear and normal impact loadings on one face of a narrow slit. *Int. J. Solids Struct.* **18**, 467–477 (1982).
11. L. M. Brock and Y. C. Deng, Dynamic studies of half-plane and cruciform cracks. *Int. J. Eng. Sci.* **18**, 163–171 (1985).
12. L. M. Brock, Nonuniform edge dislocation motion along an arbitrary path. *J. Mech. Phys. Solids* **31**, 123–132 (1983).
13. L. M. Brock, Dynamic analysis of nonsymmetric problems for frictionless indentation and plane crack extension. *J. Elasticity* **8**, 273–283 (1978).
14. F. Erdogan and G. D. Gupta, On the numerical solution of singular integral equations. *Q. Appl. Math.* **30**, 525–534 (1972).
15. G. Carrier, M. Krook and C. Pearson, *Functions of a Complex Variable*. McGraw-Hill (1966).
16. A. Ralston, *A First Course in Numerical Analysis*. McGraw-Hill (1965).
17. L. M. Brock, Two basic problems of plane crack extension: a unified treatment. *Int. J. Eng. Sci.* **15**, 527–536 (1977).
18. I. N. Sneddon and M. Lowengrub, *Crack Problems in the Classical Theory of Elasticity*, Wiley, New York (1969).
19. J. D. Achenbach and L. M. Brock, Rapid extension of a crack. *J. Elasticity* **1**, 56–63 (1971).
20. K. B. Broberg, The propagation of a brittle crack. *Ark. Fys.* **18**, 159–192 (1960).